Pol. J. Environ. Stud. Vol. XX, No. X (XXXX), 1-14
DOI: *10.15244/pjoes/220636* ONLINE PUBLICATION DATE: 2026-09-18

Original Research

Spatiotemporal Variation in Soil Erosion and Its Drivers in Guizhou: A RUSLE-Based Analysis

Tao Chen[1,2#*], Man Li[1,3#], Zhonghua He[1], Kun Yang[2***], Mei Yang[1], Yuanyi Jiang[2], Hong Wang[2], Haixiang Guo[2]**

[1]School of Geography and Environmental Science, Guizhou Normal University, Guiyang 550025, China
[2]Guizhou Provincial Archives of Surveying and Mapping Data, Guiyang 550004, China
[3]Key Laboratory of Remote Sensing Applications in Mountain Resources and Environment, Guiyang 550025, China

Received: 14 October 2025
Accepted: 13 April 2026

Abstract

Research on regional soil erosion under global climate change has attracted widespread attention. Soil erosion in Guizhou Province, China, is severe due to the presence of extensively developed karst formations, making it a major local ecological issue. In this context, the present study aims to calculate the soil erosion modulus in Guizhou Province using the Revised Universal Soil Loss Equation (RUSLE) and to assess its spatiotemporal variation characteristics. In addition, the relationships between soil erosion and rainfall and vegetation coverage from 2000 to 2020 were further explored in this study. The results showed that: (1) From 2000 to 2020, soil erosion in Guizhou Province was at low levels. There was a significant linear increase in the average annual soil erosion modulus, with a change rate of 0.0001 t/(hm²·a) ($P<0.05$). (2) The conversion between the different soil erosion levels over the study period was generally manifested as a shift from low-level erosion (very slight, slight, and moderate erosion) to high-level erosion (severe, very severe, and extremely severe erosion). Specifically, from 2000 to 2010, high-level erosion tended to shift to low-level erosion. From 2010 to 2020, on the other hand, low-level erosion shifted to high-level erosion. (3) Rainfall was the dominant factor affecting soil erosion changes in Guizhou Province from 2000 to 2020, while improvements in vegetation conditions played a major role in reducing the soil erosion modulus.

Keywords: rainfall erosivity, soil erodibility, NDVI, soil erosion levels, Guizhou Province of China

Introduction

Regional soil erosion in the context of global climate change has attracted great attention from researchers worldwide in recent years [1, 2]. Guizhou Province, Southwest China, is one of the regions with the most typical karst-landform development in the world, where the exposed karst area accounts for 61.92% of the province's total area. Furthermore, this province is characterized by the presence of the largest area of rocky

# equal contribution
*e-mail: chentao311@gznu.edu.cn
**e-mail: hezhonghua7621@126.com
***e-mail: yangkungis@163.com

desertification in China. Guizhou Province has long been underdeveloped, with relatively low economic growth and severe ecological damage. The presence of shallow soil layers caused by the distinctive dual structure of karst landforms, together with the occurrence of concentrated rainfall in the province, leads to severe soil and water loss [3, 4]. Guizhou Province is also a priority area for controlling soil and water loss in China [5, 6]. The assessment of spatiotemporal variability and characteristics of soil erosion in Guizhou Province under current climate change conditions is, therefore, of significant theoretical and practical value for developing soil and water loss control strategies and implementing effective ecological conservation measures.

Soil erosion can lead to severe environmental issues, including decreased soil fertility and land degradation [7, 8]. The Revised Universal Soil Loss Equation (RUSLE) has been widely applied in soil erosion studies due to its simplicity and ease of use [9, 10]. The RUSLE model considers five factors, namely rainfall erosivity, soil erodibility, slope length and steepness, vegetation cover, and soil-water conservation measures [11, 12]. In fact, the occurrence of frequent and extreme regional rainfall events in recent years as a result of global climate change has increased rainfall erosivity. Ma et al. (2024) argued that human activities were the main factor controlling soil erosion changes in Yunnan Province, China, followed by climate change [13]. Zhang et al. (2024) suggested that the increase in soil erosion in the Jiuyuangou Watershed of the Loess Plateau was attributed to an increase in erosive rainfall events, as well as to the unreasonable allocation of land use to some extent [14]. Abdi et al. (2023) stated that extreme erosive rainfall events were the major driver of the increased soil erosion in the Shaqlawa agricultural area of the Kurdistan Region, Iraq [15].

Soil erodibility is controlled by soil texture and is closely related to other factors such as soil type. Slope length and steepness (topographic factors) can exhibit relatively slight spatiotemporal variability. Tsegaye et al. (2024) concluded that soil erodibility was the dominant factor in the soil erosion process of the Fakisi Watershed in the Abbay Basin, Ethiopia [16]. Mengie et al. (2022) found that areas with high soil erosion rates in the Tashat Watershed, northwestern Ethiopia, were distributed in regions with steep slopes and erosion-prone soil types [17]. Soil-water conservation practice and vegetation cover factors can be extracted from DEM (Digital Elevation Model) and NDVI (Normalized Difference Vegetation Index), respectively, or obtained using assignment methods [18-22]. The principle of assignment methods is to assign a value of 0 to identified terraced fields [20, 23].

Land management and vegetation cover change are important driving factors of soil erosion. Schwamback et al. (2024) argued that different land cover types lead to significant differences in soil loss rates. They showed a 20-fold and a five-fold increase in soil runoff and soil loss, respectively, following the conversion of forests to pastures or sugarcane fields [24]. Li et al. (2024) simulated the relationship between potential vegetation dynamics and soil erosion in the Loess Plateau from 1982 to 2016 and demonstrated the enhancing impacts of vegetation restoration on soil conservation capacity by an average value of 84% per year [25]. Mathewos et al. (2024) found that the expansion of cultivated land, construction land, and bare land in the Boyo Watershed of the Central Rift Valley Basin over the 1991-2020 period has led to annual increases in soil loss of 15.5, 35.9, and 38.3 t/(hm^2·a), respectively, compared with forests, water bodies, wetlands, and grasslands [26]. Ma et al. (2024) suggested that vegetation changes in the Zhifanggou Watershed on the Loess Plateau contributed to 86.10% of soil erosion in 2022 [27]. Ma et al. (2025) stated that improving vegetation coverage could effectively mitigate the risk of soil and water loss in the urban agglomerations of Central Yunnan, China [28]. Yi et al. (2024) highlighted an increased soil erosion risk in the middle and lower reaches of the Yangtze River, China, as a result of urban expansion-associated decline in vegetation. Specifically, a 6.4% reduction in the vegetation cover coefficient led to a 3.7% increase in the potential soil erosion risk [29]. The above-mentioned RUSLE-based studies demonstrated the complexity of the soil erosion process, which is characterized by significant spatial heterogeneity. Furthermore, they showed the regional differences in the relative contributions of the various RUSLE factors to soil erosion.

As a region that is severely affected by soil and water loss, extensive research has been conducted on soil erosion in Guizhou Province. For example, Gao et al. (2024a; 2024b) studied soil erosion in Guizhou Province and Bijie Prefecture, highlighting the role of human activities, including the Grain for Green Project and Rocky Desertification Control, in reducing soil erosion [30]. They also argued that the increase in rainfall erosivity had led to an overall rise in soil erosion in Guizhou Province, mitigating the role of human activities in soil erosion control [31]. Jian et al. (2025) suggested that different soil erosion prevention and control strategies in Guizhou Province should be adopted based on karst landform types and land use patterns [32]. Guo et al. (2024) concluded that elevation was the dominant factor influencing soil erosion on the Yunnan-Guizhou Plateau, where Yunnan Province and Guizhou Province, China, are located [33]. Additionally, some scholars have highlighted an increasing trend in rainfall erosivity in Guizhou Province [34-36].

High-resolution data products based on Landsat images have become increasingly available in recent years, such as 30 m-resolution NDVI data. These products have improved the ability to conduct soil erosion research using high geospatial resolution data. Indeed, soil erosion data at 30 m-resolution can provide more detailed information compared to those with large spatial resolutions (e.g., 1 km, 500 m, and 250 m). In this context, the present study aims to calculate the soil

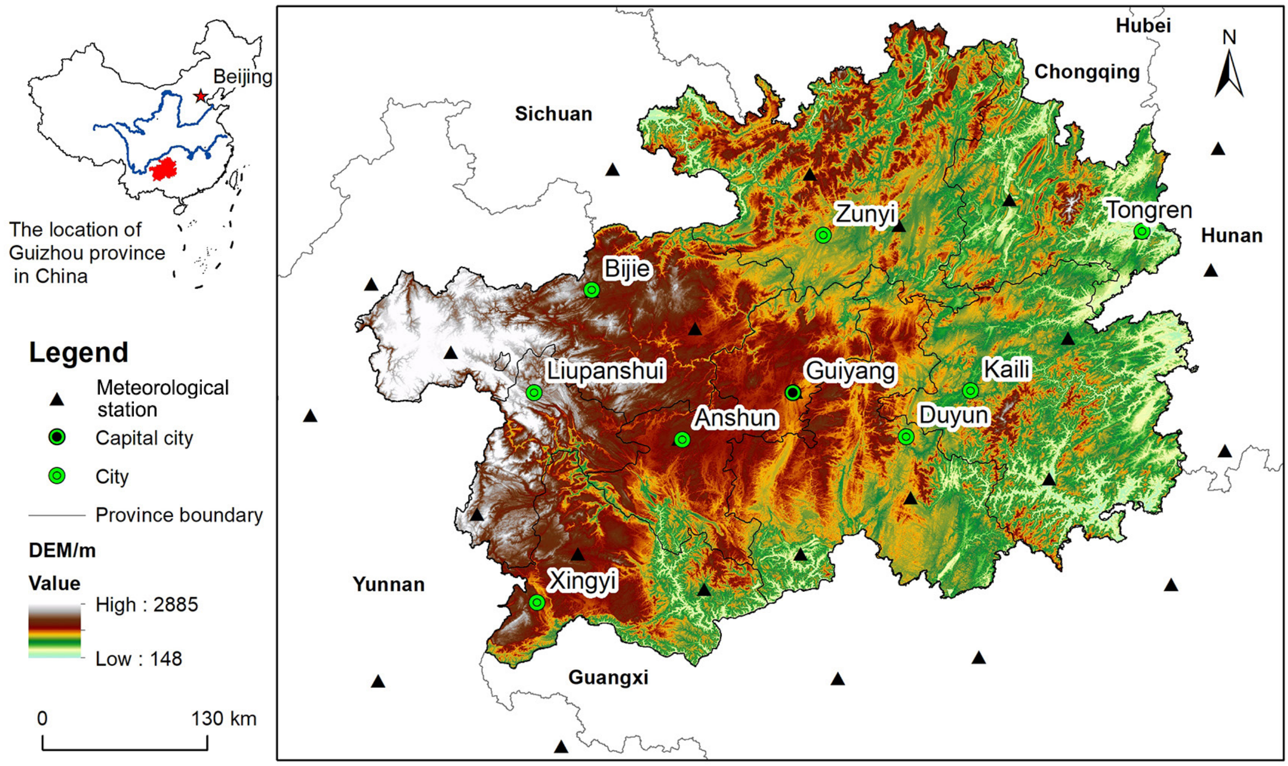

Fig. 1. Geographic locations of the study area and meteorological stations.

erosion modulus of Guizhou Province from 2000 to 2020 using the RUSLE method combined with soil texture and DEM data. Additionally, the spatiotemporal variability of the soil erosion modulus and its relationships with long-term rainfall and vegetation data (2000-2020) from 29 meteorological stations and 30 m-resolution Landsat NDVI data, respectively, were further explored. The findings of this study provide scientific support for understanding the spatiotemporal variability of soil erosion in Guizhou Province, as well as for guiding ecological protection and restoration policies.

Materials and Methods

Study Area

Guizhou Province is located in the southwestern part of China, with its geographical coordinates ranging from 103°36′17.60″E to 109°36′14.39″E in longitude and from 24°37′12.40″N to 29°12′2.70″N in latitude. It borders Hunan Province to the east, the Guangxi Zhuang Autonomous Region to the south, Yunnan Province to the west, and Sichuan Province and Chongqing Municipality to the north, covering a total land area of 176,100 km² (Fig. 1). Geomorphologically, the province belongs to the Yunnan-Guizhou Plateau. The terrain within its borders is higher in the west and lower in the east, sloping northward, eastward, and southward from the central part, with elevations ranging from 148 to 2,885 m. It is characterized by a subtropical humid monsoon climate. Specifically, the average annual air temperature and precipitation over the 1990-2020 period were 16.31°C and 1,194.13 mm, respectively. The rainy and hot seasons coincide, with precipitation concentrated in summer and spring. The major soil types in Guizhou include yellow, red, yellow-brown, calcareous, purple, paddy, and mountain meadow soils. Influenced by its latitudinal location and topographic distribution, there are diverse vegetation types in the province, including tropical and subtropical vegetation (e.g., monsoon and evergreen broad-leaved forests), as well as temperate and cold-temperate vegetation (e.g., deciduous broad-leaved and subalpine coniferous forests). On the other hand, the study area includes numerous rivers belonging to two major river systems, namely the Yangtze River and the Pearl River. The province serves as an important ecological barrier and water conservation area for the tributaries of the Yangtze River and the upper reaches of the Pearl River. However, it faces relatively severe soil erosion due to the widespread and well-developed karst landforms and the occurrence of extreme rainfall events, making it a key region for soil erosion control in China.

Materials

The data used in the study included:

(1) Daily precipitation data for the 2000-2020 period were obtained from 29 meteorological stations in Guizhou Province and its surrounding areas. The spatial distribution of these stations is shown in Fig. 1. The data

were downloaded from the National Meteorological Science Data Center (data.cma.cn).

(2) 1-km raster soil texture data for China were downloaded from the Food and Agriculture Organization of the United Nations (www.fao.org), including soil texture fractions (clay, silt, sand contents) and soil organic matter content.

(3) Topographic factor (*LS*): a global topographic (*LS*) factor dataset with a 30 m resolution [37] was downloaded from the National Earth System Science Data Center, National Science & Technology Infrastructure of China (http://www.geodata.cn).

(4) An annual Landsat NDVI dataset of China, with a 30 m resolution, covering the 2000-2020 period, was generated using the annual pixel-wise maximum value composite method [38]. The data were downloaded from the National Ecological Science Data Center, National Science & Technology Infrastructure of China (http://www.nesdc.org.cn).

(5) DEM data: SRTM DEM data with a 90 m resolution were downloaded from the Geospatial Data Cloud (www.gscloud.cn).

(6) Vegetation type data: 1-km resolution raster data on the vegetation types in the province.

(7) Vector boundary of Guizhou Province. Both (6) and (7) were downloaded from the Resource and Environmental Science Data Platform (www.resdc.cn).

Previous comparative studies have shown that the spline function interpolation method outperforms the inverse distance weighting (IDW) and kriging methods in spatial interpolations of precipitation data [39]. Nevertheless, the IDW and kriging interpolation methods remain the most widely used [5, 40-42]. In this study, the IDW interpolation method, with simple calculations, was employed to map the spatial distributions of rainfall erosivity in Guizhou Province from 2000 to 2020. The soil texture data were used to calculate the soil erodibility factor, while the NDVI data were employed to calculate the 2000-2020 vegetation coverage factor. The DEM data were used to calculate the soil-water conservation measure factor. The soil erodibility, soil-water conservation measure, and vegetation type data were resampled to a 30 m resolution for subsequent analysis using the Nearest Neighbor (NN) method. This method was selected because of its high computational efficiency and ability to preserve initial data values, particularly at large scales.

Methods

The soil erosion modulus in the study area was determined using the RUSLE method, which reflects the relationships between soil erosion and rainfall, soil type, topography, vegetation coverage, and soil-water conservation measures. The RUSLE method was computed using the following formula [43]:

$$\mathrm{A} = R \times K \times L \times S \times C \times P \tag{1}$$

where A denotes the annual soil erosion modulus, t/(hm²·a); *R* denotes the rainfall erosivity factor; *K* represents the soil erodibility factor; *L* is the slope length factor; *S* is the slope steepness factor; *C* is the vegetation coverage factor; and *P* is the soil-water conservation measure factor.

(1) Rainfall erosivity (*R*)

The daily rainfall erosivity was calculated using the collected daily rainfall data according to the method proposed by Xie et al. (2016) [44]. The annual rainfall erosivity was then obtained by summing the daily rainfall erosivity values, as follows:

$$R_d = \alpha P_d^{1.7265} \tag{2}$$

where R_d is daily rainfall erosivity, MJ·mm/(hm²·h·a); P_d is daily precipitation ≥ 10 mm; *a* is a constant, set at 0.3937 in the warm season (May-September) and 0.3101 in the cold season (October-April of the following year).

(2) Soil erodibility (*K*)

The *K* factor was calculated based on the soil texture and organic carbon data for Guizhou Province, obtained from the Harmonized World Soil Database (HWSD), using the method proposed by Sharpley et al. (1990) [45], as follows:

$$\begin{aligned} K = & \{0.2 + 0.3\exp[0.0256M(1 - F/100)]\} \times [F/(F+N)]^{0.3} \\ & \times \{1.0 - 0.25T[T + \exp(3.72 - 2.95T)]\} \\ & \times \{1.0 - 0.7\delta/[\delta + \exp(-5.51 + 22.9\delta)]\} \end{aligned} \tag{3}$$

where *M*, *F*, and *N* denote the mass fractions of sand, silt, and clay in the soil, respectively (%); *T* denotes the mass fraction of soil organic carbon (%); δ = 1−*M*/100. The calculated *K* value was converted to the international system of units by multiplying it by 0.1317.

(3) Topographic factor (*LS*)

The *LS* was obtained by clipping the aforementioned 30 m-resolution global *LS* data product using the vector boundary of Guizhou Province.

(4) Vegetation coverage factor (*C*)

The *C* factor was calculated using the Landsat NDVI data according to the method proposed by Li and Zheng (2012) [46], as follows:

$$C = \exp\left(-2 \times \frac{NDVI}{1 - NDVI}\right) \tag{4}$$

where *C* denotes the vegetation coverage factor.

(5) Soil-water conservation measure factor (*P*)

The *P* factor was calculated using the method proposed by Lufafa et al. (2003) [47], based on the DEM data with a 90 m resolution, according to the following formula:

$$P = 0.2 + 0.03\theta \tag{5}$$

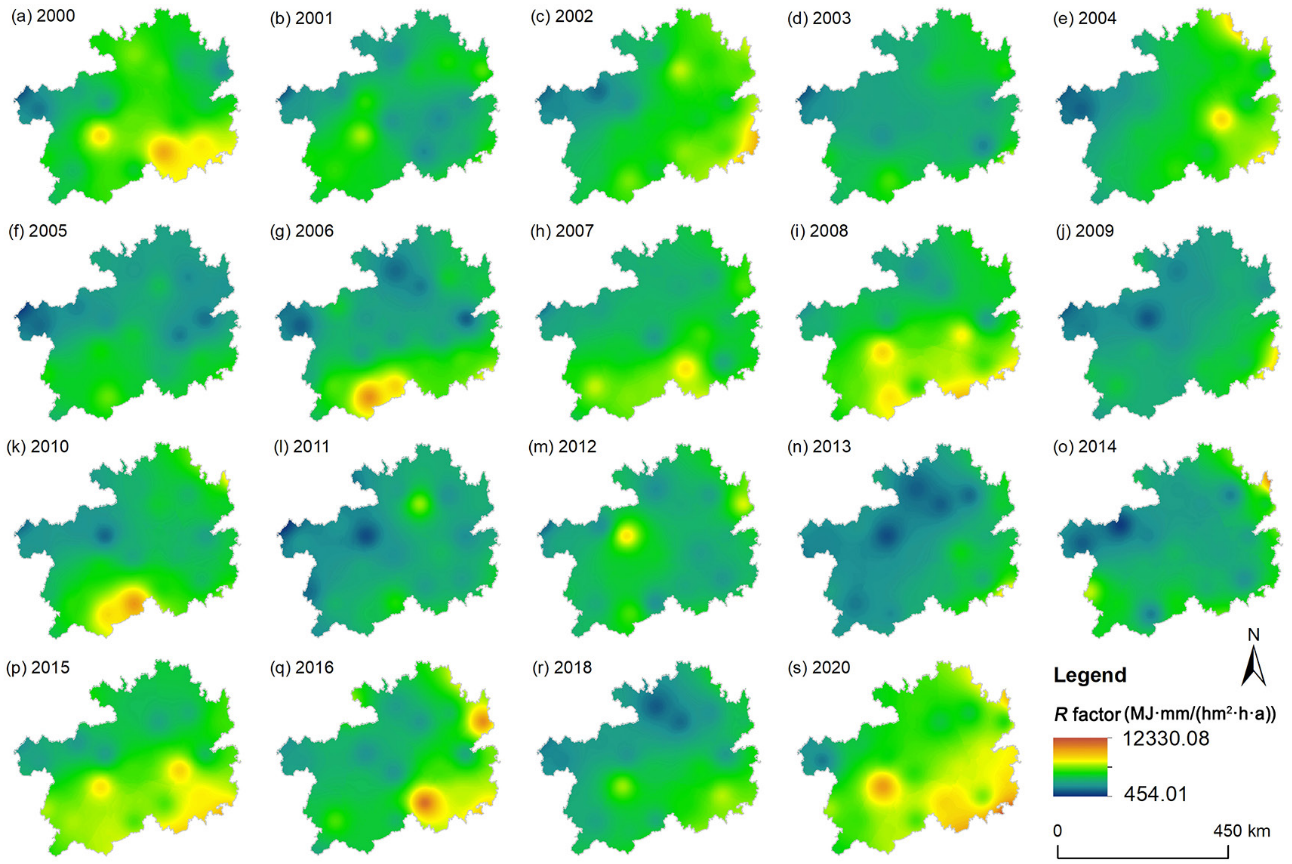

Fig. 2. Spatial distribution of *R* factor values in Guizhou Province from 2000 to 2020.

where *P* is the soil-water conservation measure factor; θ is the slope gradient (%).

Results and Discussion

Soil Erosion Factor Calculation

The results showed a close relationship between the *R* and precipitation data. Guizhou Province, located in the subtropical zone, is characterized by high rainfall amounts and a high probability of erosive rainfall events, resulting in relatively high rainfall erosivity values. The *R* values of Guizhou Province ranged from 454.01 to 12,330.08 MJ·mm/(hm²·h·a) over the 2000-2020 period. The highest values were found in the southeastern and southern parts of the province, while the lowest values were observed in the northwestern and northern parts (Fig. 2).

The average annual rainfall erosivity for Guizhou Province from 2000 to 2020 was estimated at 4,432.12 MJ·mm/(hm²·h·a). The maximum rainfall erosivity values in 2000, 2010, and 2020 were 9,533.12, 10,044.80, and 12,330.80 MJ·mm/(hm²·h·a), respectively. Xu et al. (2005) revealed that an average annual rainfall erosivity in Guizhou Province from 1951 to 2001 was 4,383.34 MJ·mm/(hm²·h·a), with a variation range of 1,865.15 to 7,238.53 MJ·mm/(hm²·h·a) [34]. Dai et al. (2013) estimated that the average annual rainfall erosivity in Guizhou Province from 1956 to 2000 was 5,299.80 MJ·mm/(hm²·h·a), with a range of 3,051.00 to 8,801.60 MJ·mm/(hm²·h·a) [35]. Whereas Ruan et al. (2020) indicated that an average annual rainfall erosivity in Guizhou Province from 1966 to 2017 of 4,994.22 MJ·mm/(hm²·h·a), with a range of 2,767.46 to 6,921.73 MJ·mm/(hm²·h·a) [36]. These findings were, in fact, consistent with the results revealed in this study. In contrast, Gao et al. (2024b) indicated the maximum values of rainfall erosivity in Guizhou Province in 2000, 2010, and 2020 of only 2,331.38, 2,777.36, and 2,787.82 MJ·mm/(hm²·h·a), respectively, showing relatively low rainfall erosivity levels [31]. The relatively similar findings of this study to those reported in previous related studies might be attributed to the same source of the daily precipitation data (the National Meteorological Science Data Center). On the other hand, Gao et al. (2024b) used daily precipitation data from the National Climatic Data Center (NCDC) of the U.S. National Oceanic and Atmospheric Administration (NOAA) [31]. The rainfall erosivity calculation results of this study suggest greater soil erosion modulus values than those reported by Gao et al. (2024b) [31]. However, the above-mentioned comparative analysis results suggest basically accurate rainfall erosivity calculations in this study.

The *K* factor reflected the likelihood of soil erosion under the impacts of rainfall events, from the

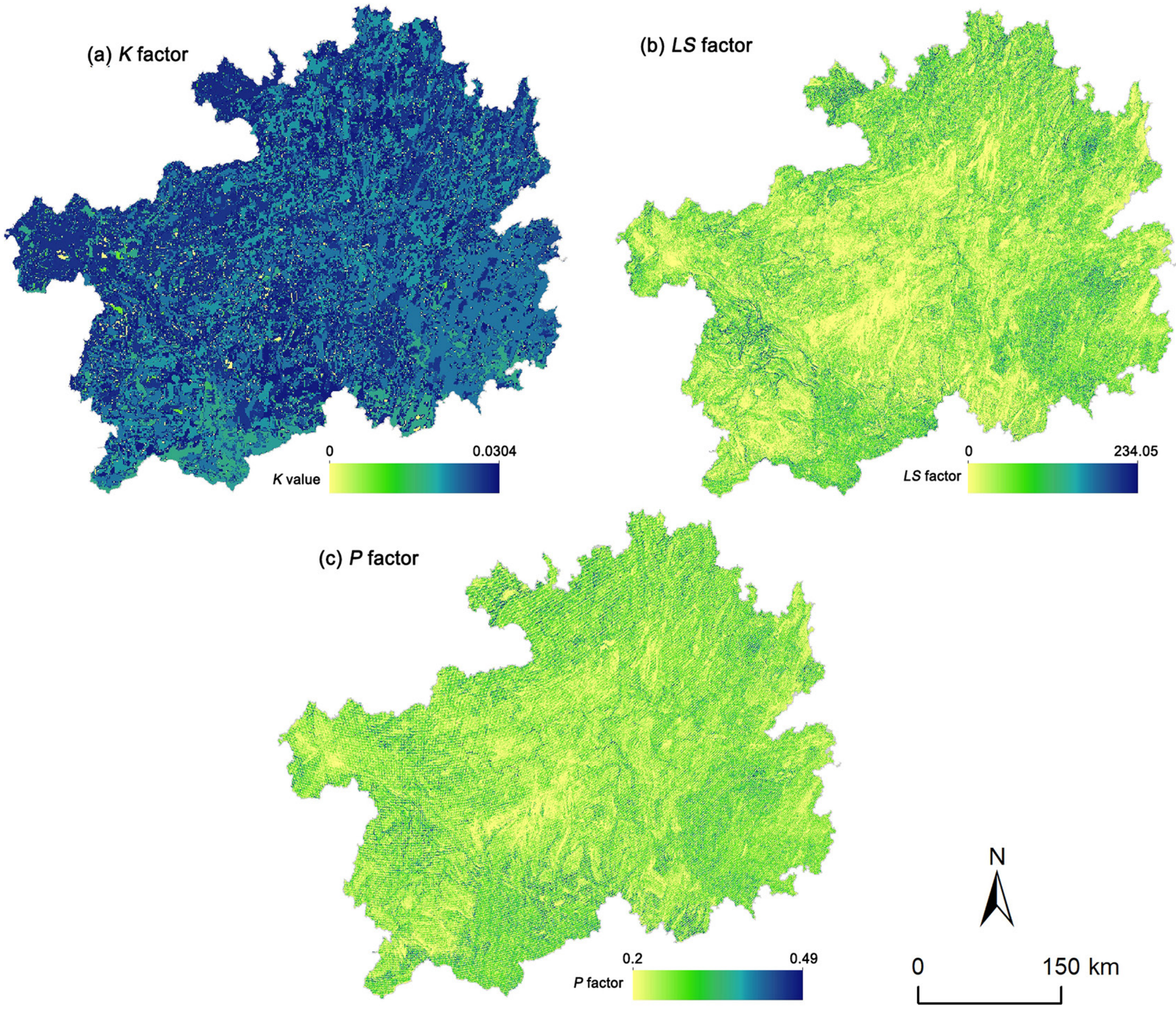

Fig. 3. Spatial distributions of the a) *K*, b) *LS*, and c) *P* factors in Guizhou Province.

perspective of soil texture. In this study, the *K* factor in Guizhou Province ranged from 0 to 0.0304. Because the province is dominated by mountains, the distribution of soil types is relatively complex. Overall, the high-*K* value areas were distributed in the western and northern parts of the province, while the low-*K* value areas were found in the southern and eastern parts (Fig. 3a)).

The *LS* factor can influence eroded soil materials moving along the slope after the occurrence of soil erosion. In fact, soil erosion can exhibit increasing-decreasing trends with increasing slope steepness, while slope length has a significant impact on the migration of eroded soil materials. In other words, the longer the slope length, the lower the probability that eroded soil materials enter the gullies. The *LS* factor in Guizhou Province ranged from 0 to 234.05, with high- and low-value areas distributed in the peripheral and central parts of the province, respectively (Fig. 3b)).

In this study, the *P* factor values ranged from 0.2 to 0.49. Their spatial distribution in the province was consistent with that of the LS factor values (Fig. 3c)).

The *C* factor reflects the effect of vegetation on erosive rainfall: the better the vegetation condition in an area, the lower the likelihood of soil erosion. In this study, the *C* values in Guizhou Province ranged from 0 to 1 over the 2000-2020 period, showing a temporally increasing trend during this period (Fig. 4). This finding might be related to human activities driven by the rapid economic development of the province, such as urban expansion, road construction, and mining activities. Specifically, these human activities led to the deterioration of vegetation conditions, which in turn increased soil erosion.

The soil erosion modulus values for Guizhou Province from 2000 to 2020 ranged from 0 to 3,252.96 t/(hm²·a). The spatial distribution of the soil erosion modulus was relatively scattered due to the 30-m spatial resolution of the data (Fig. 5). The average soil erosion modulus values in the Bijie area and the entire Guizhou Province in 2020 were 48.67 t/(hm²·a) [30] and 5.81 t/(hm²·a) [31], respectively. In contrast, the calculated average soil erosion modulus in Guizhou Province

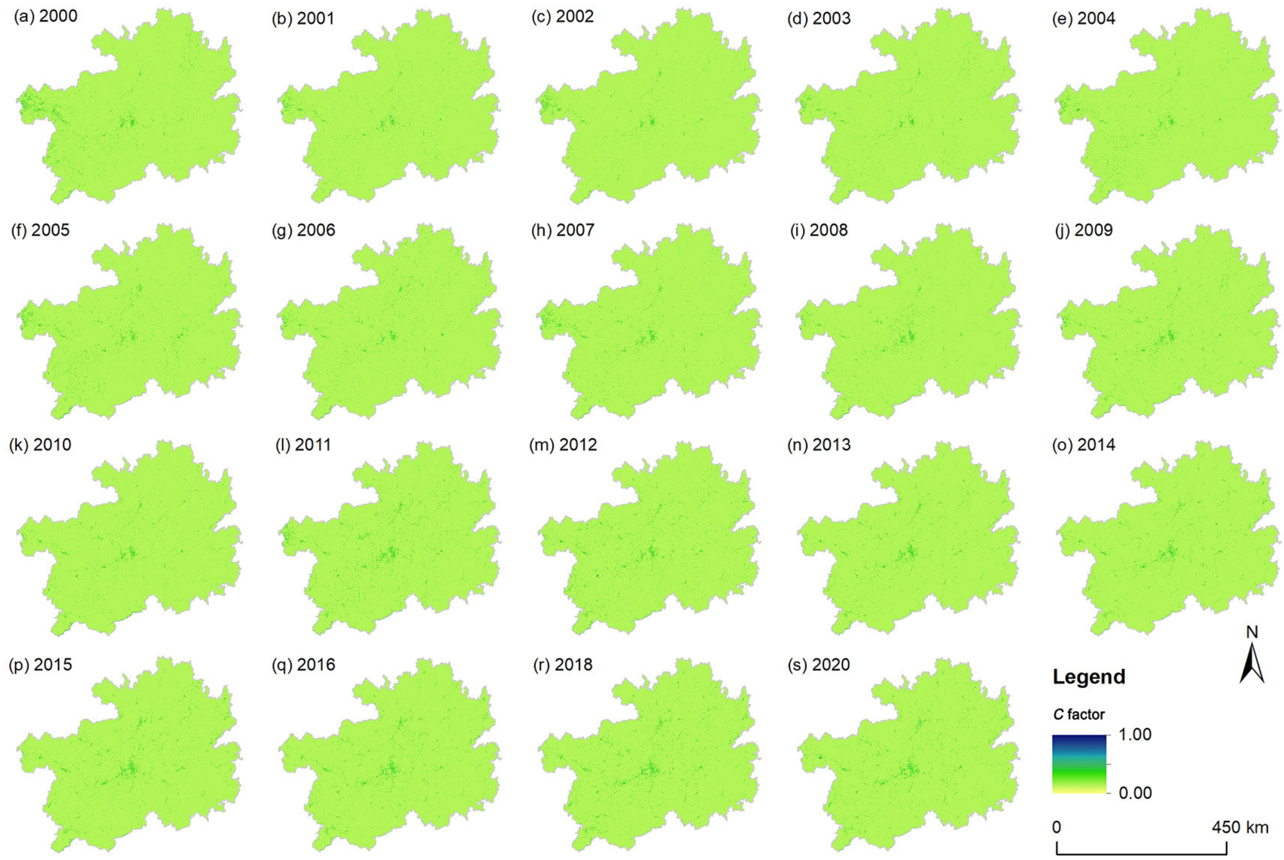

Fig. 4. Spatial distributions of the C factor in Guizhou Province during 2000-2020.

in this study was 76.27 t/(hm²·a) in 2020, indicating an overestimation of the soil erosion modulus. This is attributed to the limitations of the RUSLE application in karst landforms, neglecting the underground seepage in karst regions and the impacts of rock clast distribution on soil erodibility and topographic factors. This can lead to the overestimation of soil erosion modulus in the study area. Meanwhile, the "salt-and-pepper noise" arising from the use of 30 m-resolution NDVI data might result in discontinuous and fragmented spatial distribution of soil erosion modulus, negatively affecting the soil erosion assessment results.

Temporal Variability of Soil Erosion

Temporal Variability of the Annual Average Soil Erosion Modulus

The average annual soil erosion modulus values in Guizhou Province increased from 65.22 to 76.27 t/(hm²·a) over the 2000-2020 period, showing an overall significant linear increasing trend with a change rate of 0.0001 t/(hm²·a) per year ($P<0.05$). The variability consisted of decreasing-increasing stages. Specifically, the first stage was from 2000 to 2013, during which the average soil erosion modulus decreased from 65.22 to 37.58 t/(hm²·a), corresponding to a reduction rate of 42.37%. The second stage, on the other hand, was found from 2013 to 2020, showing an increasing trend in the average soil erosion modulus, which increased from 37.58 to 76.27 t/(hm²·a), accounting for an increasing rate of 102.92% (Fig. 6).

Area Change of Different Soil Erosion Levels

In this study, soil erosion was classified into six levels based on the thresholds of 1000, 2000, 5000, 8000, and 15000 t/(km²·a) and according to the Standards for Classification and Grading of Soil Erosion (SL190-2007) [48, 49]. These classes included the very slight, slight, moderate, severe, very severe, and extremely severe erosion classes. Additionally, the area proportions of the different soil erosion levels and their changes were further calculated and analyzed in this study (Fig. 7).

There were relatively slight changes in the area ratio of different soil erosion levels in Guizhou Province over the 2000-2020 period. The average annual area ratios of the very slight, slight, moderate, severe, very severe, and extremely severe erosion areas were 24.33, 11.46, 23.77, 15.45, 17.01, and 7.98%, respectively. The six area ratios also decreased from 21.95, 9.64, 22.17, and 15.17% in 2000 to 20.09, 8.35, 20.32, and 14.49% in 2020, corresponding to change rates of -0.054, -0.034, -0.067, and -0.015%/a, respectively. In contrast, the area ratios of the very severe and extremely severe erosion classes increased from 19.84 and 11.24% in 2000 to 21.08 and

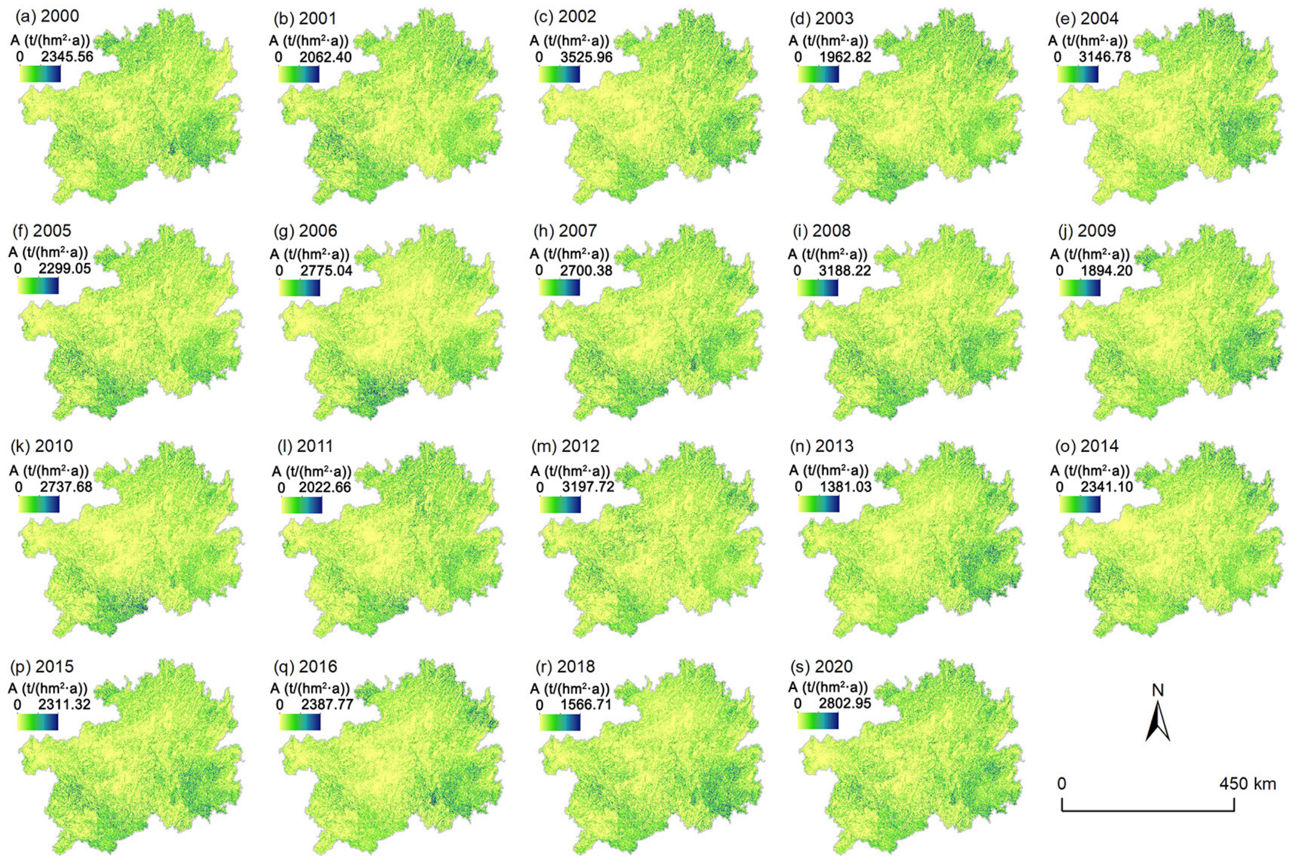

Fig. 5. Spatial distribution of soil erosion modulus (A) values in Guizhou Province during 2000-2020.

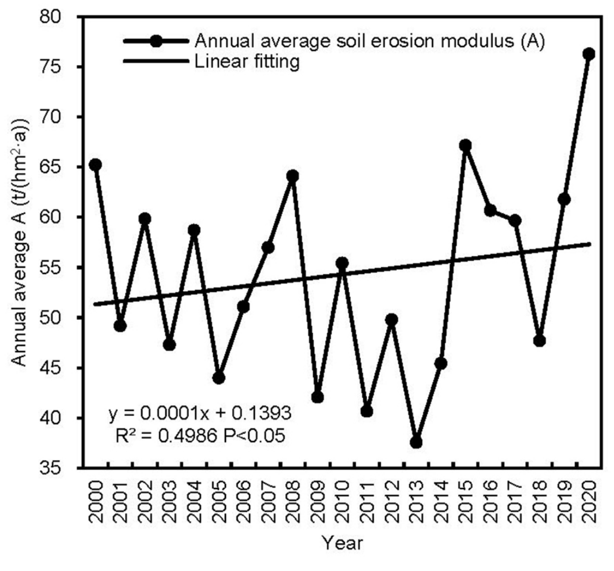

Fig. 6. Temporal changes in the soil erosion modulus (A) values in Guizhou Province from 2000 to 2020.

15.67% in 2020, with corresponding change rates of 0.033 and 0.136%/a, respectively. However, the above-mentioned change rates were statistically non-significant at the P<0.05 level, indicating that these changes were mainly dominated by fluctuations without a clear future development trend (Fig. 7).

Spatial Change in Soil Erosion

Spatial Change Process of the Different Soil Erosion Levels

Soil erosion in Guizhou Province was predominantly at the very slight, slight, and moderate erosion levels from 2000 to 2020, covering 59.55% of the provincial area. In 2000, the very slight, slight, and moderate erosion levels were mainly distributed in the central and western parts of Guizhou Province, while the severe, very severe, and extremely severe erosion levels were concentrated in the southeastern, northern, and southwestern parts of the province. The spatial distribution pattern of the different soil erosion levels was consistent from 2001 to 2020. Specifically, the very slight, slight, and moderate erosion levels generally expanded from the central part to the western and northern parts in 2001, 2003, 2005-2006, 2009, 2013-2014, and 2016. Nevertheless, Guizhou Province exhibited extensive severe, very severe, and extremely severe erosion levels in 2020 when compared with the very slight, slight, and moderate erosion levels (Fig. 8).

Transition Matrix of the Different Soil Erosion Levels

The soil erosion modulus of Guizhou Province in 2000, 2010, and 2020 was selected to compute the

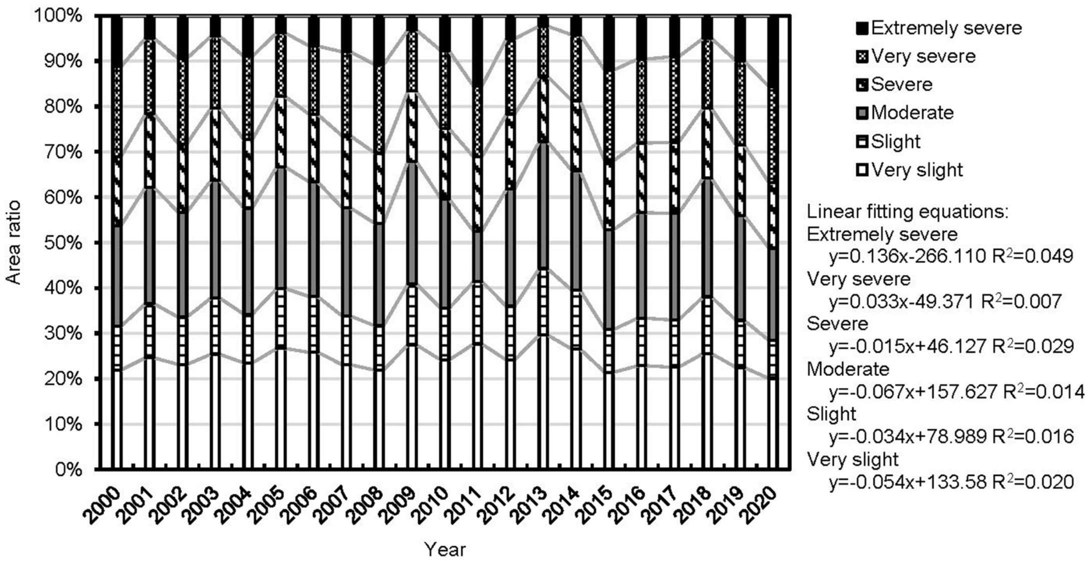

Fig. 7. Temporal changes in the area ratios of the different soil erosion levels in Guizhou Province from 2000 to 2020.

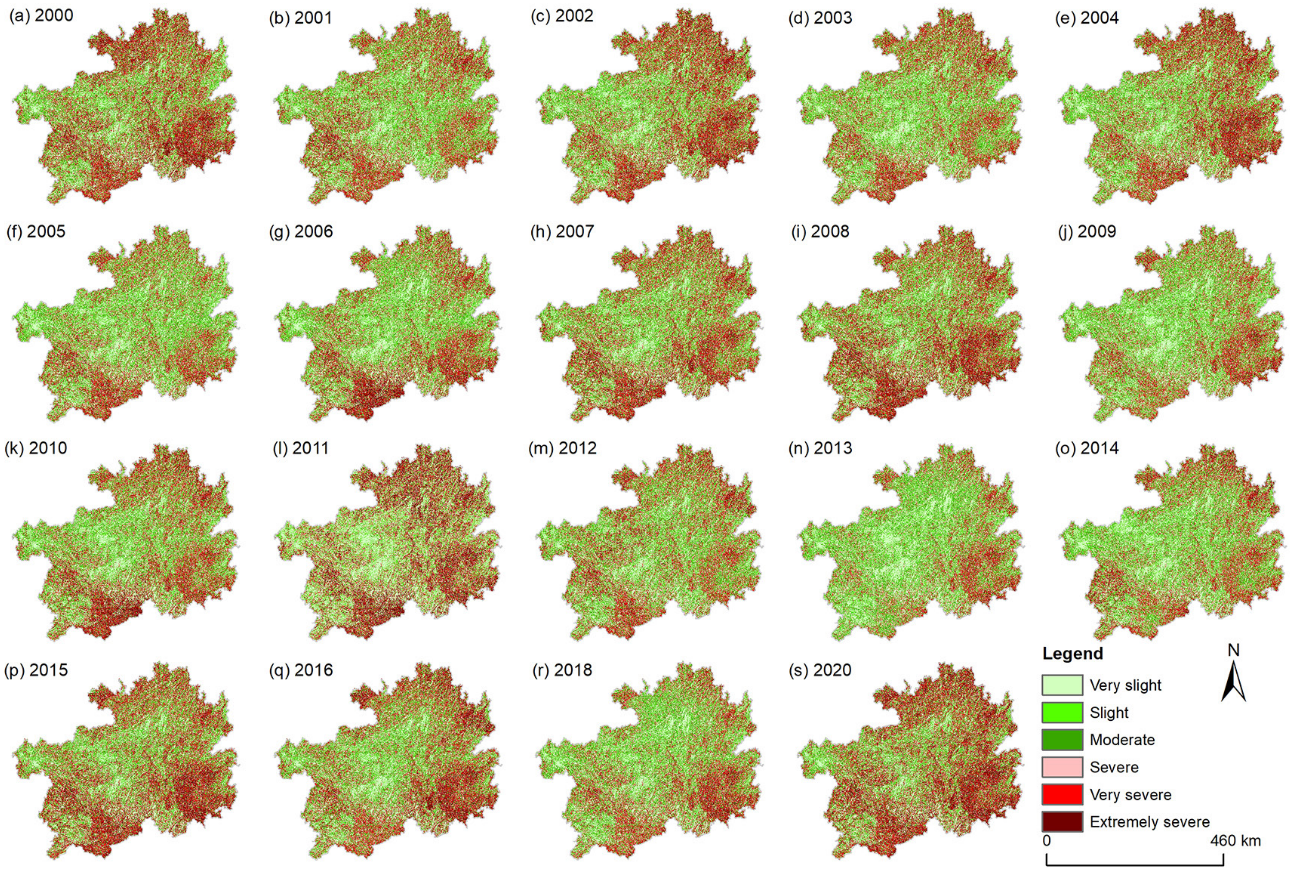

Fig. 8. Spatial distributions of the different soil erosion levels in Guizhou Province during 2000-2020.

transition matrices of areas and proportions between the different soil erosion levels in the 2000-2010, 2010-2020, and 2000-2020 periods (Table 1).

The results showed changes in the severe, very severe, and extremely severe erosion levels in Guizhou Province to the very slight, slight, and moderate soil erosion levels over the 2000-2010 period, indicating decreased soil erosion. Among the outflow areas (in 2000) of the extremely severe, very severe, severe, moderate, and slight erosion levels, the converted area of the very severe, severe, moderate, slight, and very slight erosion levels (in 2010) accounted for 97.24%,

Table 1. Area and transfer matrix-based percentages of the different soil erosion levels in Guizhou Province over the 2000-2010, 2010-2020, and 2000-2020 periods.

2000-2010		2010					
		Very slight	Slight	Moderate	Severe	Very severe	Extremely severe
2000	Very slight	—	1137.90/**95.95**/11.80	47.88/4.04/0.32	0.21/0.02/0	0/0/0	0/0/0
	Slight	4885.73/**72.89/97.11**	—	1790.94/26.72/11.97	24.67/0.37/0.15	1.92/0.03/0.02	0/0/0
	Moderate	145.12/1.26/2.88	8403.17/**73.13/87.16**	—	2700.68/23.50/16.69	230.96/2.01/1.87	11.22/0.10/0.36
	Severe	0.05/0/0	93.53/0.60/0.97	12403.05/**79.23/82.93**	—	3081.97/19.69/24.95	75.83/0.48/2.42
	Very severe	0/0/0	6.56/0.04/0.07	669.53/3.95/4.48	13243.25/**78.08/81.85**	—	3042.82/17.94/**97.22**
	Extremely severe	0/0/0	0/0/0	44.94/0.48/0.30	211.36/2.27/1.31	9035.33/**97.24/73.16**	—
2010-2020		2020					
		Very slight	Slight	Moderate	Severe	Very severe	Extremely severe
2010	Very slight	—	6786.05/**90.60/95.00**	537.88/7.34/4.14	4.48/0.06/0.02	0.10/0/0	0/0/0
	Slight	243.16/1.97/**92.79**	—	11792.18/**95.65/90.82**	251.41/2.04/1.40	41.56/0.34/0.19	0.07/0/0
	Moderate	18.88/0.10/7.21	351.38/1.79/4.92	—	16981.28/**86.40/94.59**	2184.28/1.11/9.95	119.21/0.61/0.80
	Severe	0/0/0	5.88/0.03/0.08	581.45/2.96/4.48	—	18717.80/**95.21/85.24**	354.01/1.80/2.37
	Very severe	0/0/0	0.12/0/0	71.01/0.47/0.55	679.10/4.47/3.78	—	14443.20/**95.06/96.83**
	Extremely severe	0/0/0	0/0/0	1.86/0.18/0.01	35.71/11.04/0.20	1015.86/**88.95**/4.63	—
2000-2020		2020					
		Very slight	Slight	Moderate	Severe	Very severe	Extremely severe
2000	Very slight	—	3375.62/**91.48/83.19**	310.32/8.41/4.34	4.18/0.11/0.04	0/0/0	0/0/0
	Slight	408.97/6.49/**87.28**	—	5719.91/**90.72/80.01**	163.01/2.59/1.63	13.00/0.21/0.11	0/0/0
	Moderate	59.58/0.58/12.72	674.97/6.52/16.63	—	8877.45/**85.74/88.55**	684.77/6.61/5.87	57.50/0.56/0.66
	Severe	0/0/0	7.26/0.06/0.18	870.95/7.77/12.18	—	10052.50/**89.70/86.20**	276.07/2.46/3.16
	Very severe	0/0/0	0/0/0	247.57/2.60/3.46	867.64/9.13/8.65	—	8391.95/**88.27/96.18**
	Extremely severe	0/0/0	0/0/0	0.08/0.01/0	113.08/11.04/1.13	911.06/**88.95**/7.81	—

Note: In the table, "a/b/c" represent the area (km^2), percentage relative to the area of the previous year (%), and percentage relative to the area of the subsequent year (%), respectively. The bold font indicates the higher transfer areas or the percentages of the transition matrix between the different soil erosion levels.

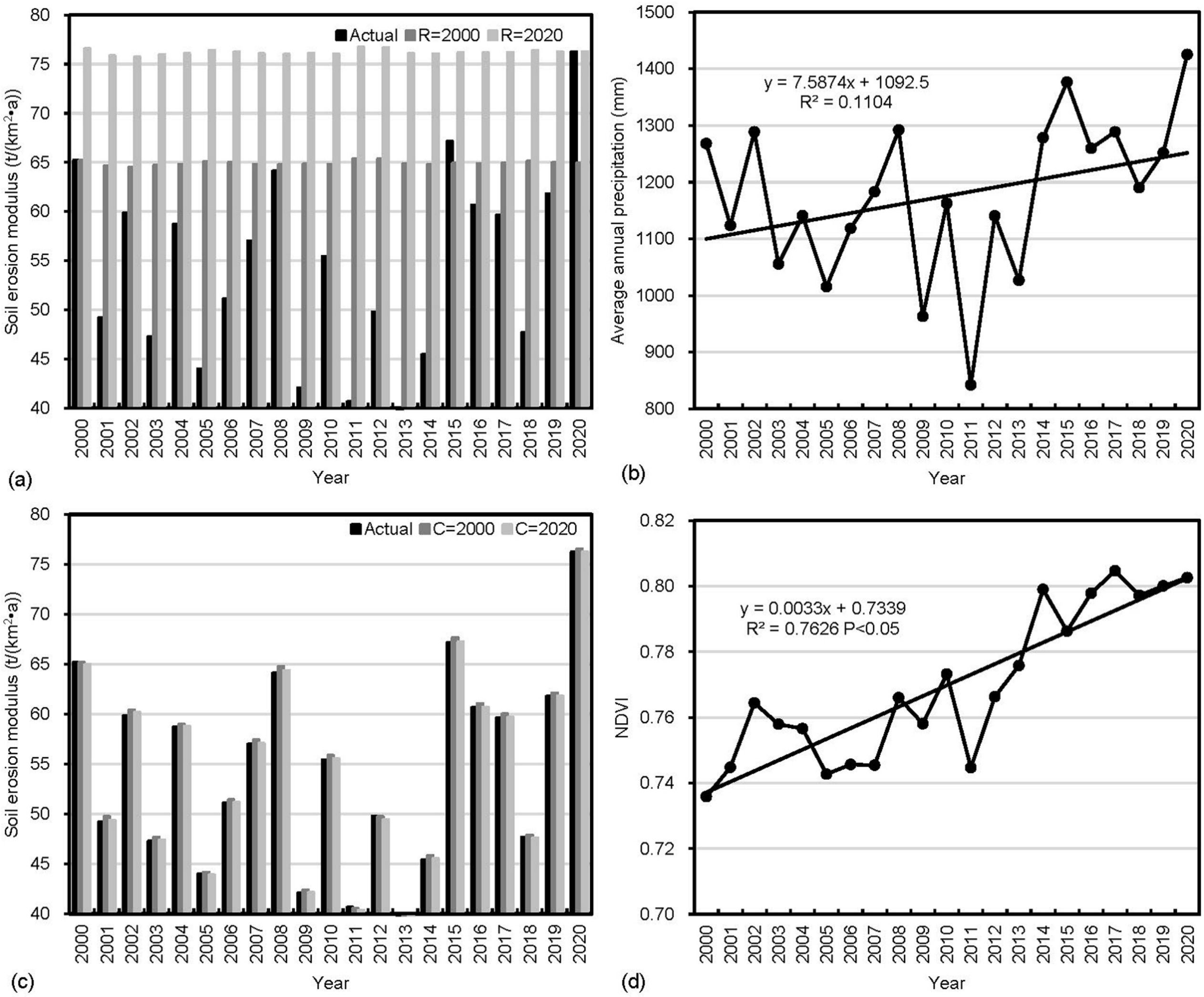

Fig. 9. Temporal variability of the soil erosion modulus under a) the unchanged precipitation and c) vegetation coverage; b) annual precipitation and d) NDVI in Guizhou Province from 2000 to 2020.
Note: The soil erosion modulus was recalculated based on a) the rainfall erosivity (R) data for 2000, 2020, and the 2000-2020 period, as well as c) using the vegetation cover factor (C) data for 2000, 2020, and the 2000-2020 period.

78.08%, 79.23%, 73.13%, and 72.89%, respectively. In contrast, among the inflow areas (in 2010) of the very severe, severe, moderate, slight, and very slight erosion levels, the percentages of the converted areas from the extremely severe, very severe, severe, moderate, and slight erosion levels were 73.16%, 81.85%, 82.93%, 87.16%, and 97.11%, respectively.

The transition between the different soil erosion levels in Guizhou Province from 2010 to 2020 was mainly from the low (very slight, slight, and moderate) to high (severe, very severe, and extremely severe) soil erosion levels, generally showing increased soil erosion. Among the outflow areas (in 2010) of the very slight, slight, moderate, severe, and very severe erosion, the percentages of the converted areas to the slight, moderate, severe, very severe, and extremely severe erosion levels (in 2020) were 92.60%, 95.65%, 86.40%, 95.21%, and 95.06%, respectively. Whereas the percentages of the converted inflow areas in 2020 from the very slight, slight, moderate, severe, and very severe erosion levels were 95.00%, 90.82%, 94.59%, 85.24%, and 96.83%, respectively.

The transitions between the different soil erosion levels in Guizhou Province over the 2000-2020 period were characterized by a shift from the low (very slight, slight, and moderate) to the high (severe, very severe, and extremely severe) soil erosion levels, indicating increased soil erosion. Among the outflow areas (in 2000) of the very slight, slight, moderate, severe, and very severe erosion levels, the percentages of the converted areas to the slight, moderate, severe, very severe, and extremely severe erosion levels (in 2020) were 91.48%, 90.72%, 85.74%, 89.70%, and 88.27%, respectively. On the other hand, the converted inflow areas from the very slight, slight, moderate, severe, and very severe erosion levels in 2020 were 83.19%, 80.01%, 88.55%, 86.20%, and 96.18%, respectively.

Relationships of Soil Erosion with Rainfall and Vegetation Changes

Contrary to rainfall erosivity and vegetation coverage, soil erodibility, slope length and steepness, and soil-water conservation measures are generally unchanged. Therefore, the rainfall erosivity and vegetation cover factor can be controlled separately. In addition, the soil erosion modulus in Guizhou Province from 2000 to 2020 can be calculated under the scenarios where rainfall erosivity and vegetation coverage remain unchanged to explore the quantitative impacts of rainfall and vegetation on soil erosion. In this context, four scenarios were considered in this study, including unchanged rainfall erosivity (recalculated soil erosion modulus separately for 2000 and 2020) (Fig. 9a)) and unchanged vegetation coverage (recalculated soil erosion modulus separately for 2000 and 2020) (Fig. 9c)).

The average annual soil erosion modulus value of Guizhou Province, calculated based on the 2000-2020 rainfall erosivity data, was 54.32 t/(hm²·a), with a wide variation range. In contrast, the average annual soil erosion modulus value, recalculated using the 2000 and 2020 rainfall erosivity data separately, exhibited relatively slight variability (Fig. 9a)), reaching 64.93 and 76.20 t/(hm²·a), respectively. These differences might be attributed to the occurrence of relatively high rainfall amounts in 2000 and 2020 (Fig. 9b)), leading to relatively high average rainfall erosivity values in these two years, and the values were 5,323.83 and 6,244.06 MJ·mm/(hm²·h·a) in 2000 and 2020, respectively, which are higher than the 2000-2020 average annual rainfall erosivity value of 4,432.12 MJ·mm/(hm²·h·a). Under stable rainfall erosivity, on the other hand, an unchanged soil erosion modulus was obtained with a relatively slight variability. Moreover, the soil erosion modulus values from 2000 to 2020 recalculated using the rainfall erosivity of 2020 and 2000 separately were higher than those determined using the 2000-2020 rainfall erosivity data (Fig. 9a)).

In this study, the changing patterns of the annual soil erosion modulus calculated based on the 2000-2020 vegetation coverage data and those determined using the vegetation coverage data for 2000 and 2020 separately were relatively similar (Fig. 9c)). Indeed, the average annual soil erosion modulus values using the vegetation coverage data for the 2000-2020 period, 2000, and 2020 were 54.32, 54.65, and 54.36 t/(hm²·a), respectively. These findings might be attributed to the significant increase in the NDVI values over the 2000-2020 period, resulting in comparatively lower soil erosion modulus. On the other hand, the lowest and highest annual NDVI values were 0.7359 and 0.8026 in 2000 and 2020, respectively (Fig. 9d)). The calculated soil erosion modulus values using the 2020 NDVI data were slightly lower than those obtained from the 2000 NDVI data (Fig. 9c)). This finding demonstrates the mitigation effects of vegetation on soil erosion. Nevertheless, these effects were weaker than those of precipitation changes.

Conclusions

(1) The average annual soil erosion modulus in Guizhou Province showed a significant linear increase over the 2000-2020 period, with a change rate of 0.0001 t/(hm²·a) ($P<0.05$). Importantly, the proportions of the very slight, slight, moderate, and severe erosion areas decreased over the 2000-2020 period, while the very severe and extremely severe erosion areas had a temporal increasing trend.

(2) From 2000 to 2020, the very slight, slight, and moderate erosion levels were found in the central and western parts of Guizhou Province, while the severe, very severe, and extremely severe levels were concentrated in the southeastern, northern, and southwestern parts of the province. However, the results showed a conversion of the soil erosion levels over the study period. Specifically, the soil erosion levels were intensified, showing the conversion of the very slight, slight, and moderate levels to the high-level erosion levels (severe, very severe, and extremely severe), except for the 2000-2010 period, which experienced a conversion of the high-level areas to the low-level areas, resulting in reduced soil erosion.

(3) Rainfall was the dominant factor affecting the spatial changes in the soil erosion levels in Guizhou Province from 2000 to 2020, whereas vegetation improvement played a secondary role in reducing the soil erosion modulus.

Regional extreme heavy precipitation events have become frequent in recent years due to the continuous impacts of global climate change. Guizhou Province is a major karst landform area facing increasingly severe soil erosion, making the implementation of prevention and control measures crucial. In fact, it is recommended to increase financial investment, strengthen soil and fertilizer conservation measures within the province, and improve vegetation coverage to effectively mitigate soil erosion. In addition, it is suggested to conduct future research on the applicability and modification of the RUSLE model in karst areas, as well as on the improvement of geospatial data resolution, to enhance soil erosion assessments.

Acknowledgements

This work was supported by the Guizhou Province Innovation Platform Project (No. Qiankehe platform CXPTXM [2025]002), the Natural and Scientific Research Fund of Guizhou Water Resources Department (No. KT202517, KT202237), the Guizhou Province Science and Technology Support Program (No. Qiankehe-SF [2023] normal 222), the Guizhou Provincial Basic Research Program (Natural Science) (No. Qiankehe base-ZK [2024] normal 445), and the Natural Science Foundation of Guizhou Province, China (No. QKHJ-ZK[2023] Key028). We thank the National Earth System Science Data Center, National Science

& Technology Infrastructure of China (http://www.geodata.cn), and the National Ecosystem Science Data Center, National Science & Technology Infrastructure of China (http://www.nesdc.org.cn), for their support in providing the LS and NDVI data.

Conflict of Interest

The authors declare no conflict of interest.

References

1. ROY S.K., MONDAL C., KARIM M., GHOSH S., KUMAR A. Utilizing GIS and remote sensing for soil loss estimation in Kopai river basin: an application of the RUSLE model. Proceedings of the Indian National Science Academy, **90** (4), 943, **2024**.
2. ABDO H.G. Estimating water erosion using RUSLE, GIS and remote sensing in Wadi-Qandeel river basin, Lattakia, Syria. Proceedings of the Indian National Science Academy, **87** (3), 514, **2021**.
3. ZHANG M.X., GU X.P., LIAO L.F., TIAN P.J. Effects of climate change and human activities on vegetation cover change in rocky desertification area of Guizhou Province. Earth and Environment, **51** (1), 76, **2023** [In Chinese].
4. LI X., YANG S.T., LUO Y., LI C.J., ZHOU B.C., LOU H.Z., ZHANG Y.J., ZHANG J. Coordinated development of economic growth and vegetation restoration in the national ecological civilization pilot zone (Guizhou). China Environmental Science, **42** (9), 4333, **2022** [In Chinese].
5. FANG F.Y., FANG Q., YU W.Y., FAN C.H., ZI R.Y., ZHAO L.S. RUSLE model evaluation of the soil and water conservation ratio of the Guizhou province in China between 2000 and 2019. Sustainability, **14** (13), 8219, **2022**.
6. YANG T.F., WU X.C., SHANG H.L., HE X. Temporal-spatial changes of soil erosion and their relation with precipitation since the project of returning farmland to forest in Guizhou Province. Carsologica Sinica, **36** (4), 478, **2017** [In Chinese].
7. PANDEY R., MEHTA D., KUMAR V., PRADHAN R.P. Quantifying soil erosion and soil organic carbon conservation services in indian forests: a RUSLE-SDR and GIS-based assessment. Ecological Indicators, **163**, 112086, **2024**.
8. DUTTA B., SRIVASTAVA P.K., BORUAH A. Quantifying soil erosion dynamics in lower Subansiri basin, Assam, India, using the RUSLE model. Journal of Sedimentary Environments, **10**, 173, **2024**.
9. NIGUSSIE A.B., AYELED G., ENDALEW A., MIHERETU B.A., AMOGNEHEGN A.E., ADAMU A.Y., KARUPPANNAN S. Integrating google earth engine and GIS for RUSLE-based soil erosion and sediment yield assessment in Borkena watershed, Ethiopia. Journal of Sedimentary Environments, **10**, 197, **2025**.
10. TAO W.H., LIU S.Y., WANG Q.J., SU L.J., SUN Y. Spatiotemporal characteristics of soil erosion on the Chinese Loess Plateau and strategies for vegetation management. Journal of Soil Science and Plant Nutrition, **24** (3), 4439, **2024**.
11. KUMAR S., SINGH D., KUMAR A., KUMAR M., GIRI K., DEVI K., SINGH S. Estimation of soil erosion in indo-gangetic region using revised universal soil loss equation (RUSLE) model and geospatial technology. Modeling Earth Systems and Environment, **9** (1), 1251, **2023**.
12. TESEMA M., FEYESSA F.F., KEBEDE A.B., GERESU B.A. Evaluation of soil erosion rate using geospatial techniques for enhancing soil conservation efforts. Environmental System Research, **13** (1), 35, **2024**.
13. MA D.L., PENG S.Y., LIN Z.Q., HUANG B.M, ZHU Z.Y., SHI S.F., GONG L.P., ZHANG R., LI T. Identification of soil erosion sensitive areas based on improved stability mapping method and the relative contributions of climate change and human activities. Ecological Indicators, **169**, 112952, **2024**.
14. ZHANG B., GUO J.L., FANG H.Y., WU S.F., FENG H., SIDDIQUE K.H.M. Soil erosion projection and response to changed climate and land use and land cover on the Loess Plateau. Agricultural Water Management, **306**, 109187, **2024**.
15. ABDI B., KOLO K., SHAHABI H. Soil erosion and degradation assessment integrating multi-parametric methods of RUSLE model, RS, and GIS in the Shaqlawa agricultural area, Kurdistan region, Iraq. Environmental Monitoring And Assessment, **195** (10), 1149, **2023**.
16. TSEGAYE L., DEGU M., MEKONNEN M., GASHAW T. Soil erosion and sediment export analysis for watershed management options in Fakisi watershed of the Abbay basin of Ethiopia. Environmental Challenges, **15**, 100948, **2024**.
17. MENGIE M.A., HAGOS Y.G., MALEDE D.A., ANDUALEM T.G. Assessment of soil loss rate using GIS-RUSLE interface in Tashat watershed, northwestern Ethiopia. Journal of Sedimentary Environments, **7** (3), 617, **2022**.
18. PAL R., HEMBRAM B., JANA N.C. Assessment of soil erosion in the Irga watershed on the eastern edge of the Chota Nagpur Plateau, India. Regional Sustainability, **5** (1), 100112, **2025**.
19. MOISA M.B., BABU A., GETAHUN K. Integration of geospatial technologies with RUSLE model for analysis of soil erosion in response to land use/land cover dynamics: a case of Jere watershed, western Ethiopia. Sustainable Water Resources Management, **9** (1), 13, **2023**.
20. SUN D.L., ZHAO W.Q., LI W., WU J.F., YANG Z.H., LV S.S. Research on soil erosion in Karst area based on GIS and RUSLE model: a case study in Guizhou province. Bulletin of Soil and Water Conservation, **36** (3), 271, **2016** [In Chinese].
21. KASHIWAR S.R., KUNDU M.C., DONGARWAR U.R. Soil erosion estimation of Bhandara region of Maharashtra, India, by integrated use of RUSLE, remote sensing, and GIS. Natural Hazards, **110** (2), 937, **2022**.
22. ARYAL K.R., PANTHI S., BASUKALA R.K., KHAREL R., GAUTAM A., POUDEL B., SHARMA S., ADHIKARI B., BUDHA R.K., KHADKA S., PARIYAR S. Soil loss estimation of Karnali river basin, Nepal. Journal of Sedimentary Environments, **8** (3), 409, **2023**.
23. WANG T. Impacts of the grain for green project on soil erosion: a case study in the Wuding river and Luohe river basins in the Shaanxi Province of China. Applied Ecology and Environmental Research, **16** (4), 4165, **2018**.
24. SCHWAMBACK D., BRANDÃÕ A.R.A., ROSALEM L.M.P., OLIVEIRA P.T.S., ANACHE J.A.A., WENDLAND E., BERNDTSSON R., PERSSON M. Land use transformations in the Brazilian Savanna: a decade of soil erosion and runoff measurements. Catena, **246**, 108412, **2024**.

25. LI P., XIE Z., YAN Z.H., DONG R.R., TANG L.H. Assessment of vegetation restoration impacts on soil erosion control services based on a biogeochemical model and RUSLE. Journal of Hydrology: Regional Studies, **53**, 101830, **2024**.
26. MATHEWOS M., WOSORO D., WONDRADE N. Quantification of soil erosion and sediment yield using the RUSLE model in Boyo watershed, central Rift valley basin of Ethiopia. Heliyon, **10** (10), e31246, **2024**.
27. MA T.L., LIU B.Y., HE L., DONG L.X., YIN B., ZHAO Y.G. Response of soil erosion to vegetation and terrace changes in a small watershed on the Loess Plateau over the past 85 years. Geoderma, **443**, 116837, **2024**.
28. MA D.L., PENG S.Y., LIN Z.Q. Towards a more comprehensive scenario analysis: response of soil erosion to future land use and climate change in the central Yunnan urban agglomeration, China. Journal of Environmental Management, **376**, 124523, **2025**.
29. YI K.X., ZHANG J.J., WANG Y.B., ZHANG S.G., LIANG S., WU G. Response of erosion sensitivity to land use change in populated areas: a case study of the middle and lower reaches of Yangtze river. Environment, Development and Sustainability, **28** (2), 3917, **2024**.
30. GAO X., YANG P.P., ZHOU Z.F., ZHU J.Q., YANG C.X. Human and natural activities: effects on soil erosion in Karst Plateau based on QAM model: a case study of Bijie city, Guizhou province, China. Land, **13** (11), 1841, **2024**.
31. GAO X., ZHOU Z.F., YANG P.P., ZHANG H.R., YANG C.X., LI S. Quantitative analysis of impact of human activities on soil erosion using the RUSLE model in a typical karst area in Guizhou, China. Environmental Monitoring And Assessment, **196** (12), 1168, **2024**.
32. JIAN S.Q., JIANG J.H., XU J., LI X.N. The interaction of factors influencing soil erosion in different karst landform types in Guizhou province, SW China. Acta Geophysica, **73** (3), 2803, **2024**.
33. GUO J.H., LIU X.H., LIU J.F., ZHANG W.B., YANG C.L., XING L.Y., LI H.Y., LUO X.P., WANG R., MAMAT Z., WANG C., ZHAO H.H. Analysis of spatial and temporal patterns of soil erosion in the Yunna-Guizhou Plateau during 2000-2030. Sustainability, **16** (17), 7769, **2024**.
34. XU Y.Q., ZHOU Q.F., LI S.C. An analysis on spatial-temporal distribution of rainfall erosivity in Guizhou province. Bulletin of Soil and Water Conservation, **25** (4), 11, **2005** [In Chinese].
35. DAI H.L., YUAN S., ZHANG K.L., ZHU Q. Study on the spatiotemporal distribution of rainfall erosivity in Guizhou province. Research of Soil and Water conservation, **20** (1), 37, **2013** [In Chinese].
36. RUAN O., LIU S.H., YANG G.B., XIE B. Spatial and temporal distribution characteristics of rainfall erosivity in Guizhou province during 1966-2017. Bulletin of Soil and Water Conservation, **40** (3), 35, **2020** [In Chinese].
37. SUN Y.W., ZHANG H.M., YANG Q.K., LI R., LIU B., ZHAO X., SHI H., LI H., REN Y., FAN X., DONG L., XU Y., CHANG Y., YUAN L. A new high-resolution global topographic factor dataset calculated based on SRTM. Scientific Data, **11** (1), 101, **2024**.
38. YANG J.L., DONG J.W., XIAO X.M., DAI J.H., WU C.Y., XIA J.Y., ZHAO G.S., ZHAO M.M., LI Z.L., ZHANG Y., GE Q.S. Divergent shifts in peak photosynthesis timing of temperature and alpine grassland in China. Remote Sensing of Environment, **233**, 111395, **2019**.
39. CAO Y.S., SUO H.Y., JIAO S.L., ZHAO Z.Q., ZHANG J., ZHAO M., LIU W., LI Y.J. Comparison of spatial interpolation methods of precipitation: a case of karst area in Guizhou province. Research of Soil and Water Conservation, **28** (1), 164, **2021** [In Chinese].
40. WU X.C., YANG T.F., SHANG H.L., HE X. Spatiotemporal characteristics of soil erosion and its response to vegetation restoration in Guizhou karst areas. Journal of Mountain Science, **21** (3), 892, **2024**.
41. WANG Z.J., LIU S.J., SU Y. Spatial-temporal characteristics of soil erosion and erosion hotspots in Guiyang city of karst plateau mountainous region in 2008-2018. Journal of Soil and Water Conservation, **34** (5), 94, **2020** [In Chinese].
42. HU X.P., ZENG C, QIAN Q.H, WANG Q., LI Y.B. Using RUSLE model to analyze temporal and spatial characteristics of soil erosion in Tongren area from 1987 to 2015. Journal of Ecology and Rural Environment, **35** (2), 158, **2019**. [In Chinese].
43. RENARD K.G., FOSTER G.R., WEESIES G., PORTER J.P. RUSLE: revised universal soil loss equation. Journal of Soil and Water Conservation, **46** (1), 30, **1991**.
44. XIE Y., YIN S.Q., LIU B.Y., NEARING M.A., ZHAO Y. Models for estimating daily rainfall erosivity in China. Journal of Hydrology, **535**, 547, **2016**.
45. SHARPLEY A.N., WILLIAMS J.R. EPIC-erosion/productivity impact calculator:1. model documentation. Technical Bulletin-United States Department of Agriculture, **4** (4), 206, **1990**.
46. LI T.H., ZHENG L. Soil erosion changes in the Yanhe watershed from 2001 to 2010 based on RUSLE model. Journal of Natural Resources, **27** (7), 1164, **2012** [In Chinese].
47. LUFAFA A., TENYWA M.M., ISABIRYE M., MAJALIWA M.J.G., WOOMER P.L. Prediction of soil erosion in a Lake Victoria Basin catchment using a GIS-based Universal Soil Loss model. Agricultural Systems, **76** (3), 883, **2003**.
48. MINISTRY OF WATER RESOURCES OF THE PEOPLE'S REPUBLIC OF CHINA (MWRPRC). SL 190-2007 Standard for classification and gradation of soil erosion. China Water & Power Press: Beijing, China, pp. 8, **2007** [In Chinese].
49. WANG, T., XU L., HU Y., ZHANG Y.P., WEI Q. Spatial and temporal changes of soil erosion in Wuding river basin, Shaanxi province, China. Research of Environmental Science, **30** (9), 1355, **2017** [In Chinese].